

1980

## Ocean Chlorophyll Studies From a U-2 Aircraft Platform

Hongsuk H. Kim

Charles R. McClain

Lamdin R. Blaine

William D. Hart

Larry P. Atkinson

*Old Dominion University*, [latkinso@odu.edu](mailto:latkinso@odu.edu)

*See next page for additional authors*

Follow this and additional works at: [https://digitalcommons.odu.edu/ccpo\\_pubs](https://digitalcommons.odu.edu/ccpo_pubs)



Part of the [Oceanography Commons](#)

---

### Original Publication Citation

Kim, H. H., McClain, C. R., Blaine, L. R., Hart, W. D., Atkinson, L. P., & Yoder, J. A. (1980). Ocean chlorophyll studies from a U-2 aircraft platform. *Journal of Geophysical Research: Oceans*, 85(C7), 3982-3990.  
doi:10.1029/JC085iC07p03982

This Article is brought to you for free and open access by the Center for Coastal Physical Oceanography at ODU Digital Commons. It has been accepted for inclusion in CCPO Publications by an authorized administrator of ODU Digital Commons. For more information, please contact [digitalcommons@odu.edu](mailto:digitalcommons@odu.edu).

---

**Authors**

Hongsuk H. Kim, Charles R. McClain, Lamdin R. Blaine, William D. Hart, Larry P. Atkinson, and James A. Yoder

## Ocean Chlorophyll Studies From a U-2 Aircraft Platform

HONGSUK H. KIM, CHARLES R. MCCLAIN, AND LAMDIN R. BLAINE

*Goddard Space Flight Center, Greenbelt, Maryland 20771*

WILLIAM D. HART

*Science Systems and Applications, Inc., Lanham, Maryland 20801*

LARRY P. ATKINSON AND JAMES A. YODER

*Skidaway Institute of Oceanography, Savannah, Georgia 31406*

Chlorophyll gradient maps of large ocean areas were generated from U-2/OCS data obtained over test sites in the Pacific and the Atlantic Oceans. The delineation of oceanic features using the upward radiant intensity relies on an analysis method which presupposes that radiation backscattered from the atmosphere and the ocean surface can be properly modeled by using a measurement made at 778 nm. The calculation of atmospheric radiance was performed by using a method developed by J. V. Dave. An estimation of the chlorophyll concentration is performed by properly ratioing radiances measured at 472 and 548 nm after removing the atmospheric effects. The correlation between the remotely sensed data and the in situ surface chlorophyll measurements has been validated in two sets of data. The results show that the correlation between the in situ measured chlorophyll and the derived quantity is a negative exponential function, and the correlation coefficient was calculated to be  $-0.965$ .

### INTRODUCTION

During the last 2 decades the space program has given us the opportunity to view the ocean from a high-altitude platform. As a result, interesting applications of remote sensing technology have emerged, one of which is the monitoring of chlorophyll pigments in the open ocean. Chlorophyll information is directly related to marine productivity, thus providing the capability of detecting locations of high biological activity. Development of operational systems which provide this information should have tremendous benefits for the harvesting and the maintenance of viable fisheries. Also, it would be extremely valuable when coupled with sea surface temperature for the oceanographic community involved in basic research.

In 1969, Clark et al. were the first investigators to measure upwelling light from an aircraft at relatively low altitudes while simultaneously obtaining measurements of chlorophyll concentrations from a surface vessel [Clark et al., 1970]. On the basis of their initial success, NASA/Goddard Space Flight Center (GSFC) in 1974 began a sensor study directed toward the development of an ocean color scanner (OCS). However, the complexities associated with the sensor development and the data analysis techniques have necessarily delayed publication of quantitative results. For instance, from the results of Clark et al. and later U-2 high-altitude flights, it became apparent that the development of reliable quantitative estimates of surface chlorophyll required that the contribution of backscattered radiation from the atmosphere and the sea surface had to be removed from the total upwelling radiance [Hovis et al., 1973]. In ensuing years, numerous field and theoretical works have been performed in an attempt to understand the various atmospheric and oceanic properties which determine the interactions between sunlight, the atmosphere, and the ocean. Although knowledge of radiative transfer in the atmosphere and especially the hydrosphere remains in-

complete, it now appears that sufficient progress has been made to enable us to provide data products useful to the oceanographic community. By far the most ambitious effort toward realization of this goal is the Nimbus-7/Coastal Zone Color Scanner (CZCS) which was launched in August 1978.

In this paper a recent OCS study is described which was initiated to prepare for a future space experiment (i.e., the space shuttle ocean color experiment scheduled for launch in 1981). In the following sections the aircraft sensor application effort, from the instrumentation to a recently successful field mission, will be discussed emphasizing the various scientific aspects which underlie this remote sensing technology. This particular exercise was a coordinated effort with a team of oceanographers who are studying interactions between the Gulf Stream and the adjacent shelf waters in the South Atlantic Bight.

### U-2 OCEAN COLOR SCANNER

A prototype OCS was built by NASA/GSFC to be mounted on a U-2 aircraft which operates at 20 km. Later, two additional units were built with slight modifications so that the second unit could be mounted on a Learjet which would fly at an altitude of 10 km, and the third on the space shuttle which, in 1981, would be operated at an altitude of 280 km. The U-2/OCS is a 10-channel scanning radiometer having a  $90^\circ$  total field-of-view and a 3.5 milliradian instantaneous field of view (IFOV). The general instrument and platform parameters are given in Table 1. The critical radiometric and spectral characteristics (i.e., spectral band, center wavelength, bandwidth, and calibration slopes) are given in Table 2.

When flown on the U-2 aircraft, the OCS swath width is 39.6 km and the footprint at nadir is approximately  $(69 \text{ m})^2$ . For comparison, the footprint of the Nimbus-7 CZCS is  $(826 \text{ m})^2$ .

U-2/OCS flight data are distributed to several investigators in the United States and western European nations. To assure

This paper is not subject to U.S. copyright. Published in 1980 by the American Geophysical Union.

TABLE 1. U-2 and OCS Parameters

Data	
Aircraft speed	201 m/s (390 knots nominal)
Air altitude	19.8 km (nominal)
Angular resolution (IFOV)	3.5 m
Footprint	69.3 × 69.3 m
FOV	±45° from nadir
Scan rate (mirror speed)	2.727 resolutions/s
Swath width	39.6 km
Output voltage	0 volts to ±5 volts
Output bandwidth	0 to 2500 Hz
Output rms noise and level	8 mV (nominal)

the radiometric accuracy of the instrument, the OCS is brought back to the laboratory approximately every 6 months for testing and calibration checks. The inspection consists of an examination of each channel with respect to its spectral position, half width, shape, and radiometric calibration. The spectral examination is carried out by using a 0.5 m Ebert spectrometer and the radiometric phase using a 1.83 m (6 foot) integrating sphere which is color corrected to approximate the sun's spectral power distribution.

The long-term stability of the large sphere is about 5%. The OCS instruments are calibrated frequently and are maintained within a 2% fluctuation limit to the sphere reading. In addition to the aforementioned calibration, the performance of the scanner also was evaluated by using sky radiance. To effect such a comparison, the downwelling intensity was measured at ground level by pointing the OCS toward the zenith, and the resulting measurements were corrected to spectral radiance values and compared with numerically calculated values. In Figure 1 a comparison of the U-2/OCS measurements with the calculated downward radiance at sea level for a clear atmosphere is shown. In the figure the intensities measured by the OCS (triangles) are compared with a theoretical spectral curve (dots and the dotted curve). The spectral characteristics of the downwelling intensities are almost defined for given atmospheric conditions by the sun's position  $\theta_s$ , the ground reflectivity  $\rho$ , and the aerosol content in the atmosphere. Especially, the blueness of the sky, or the variation of the intensity of the sky radiation, is largely influenced by the amount of aerosol present. As is shown in the figure, the majority of the measured points overlap the theoretical spectral

TABLE 2. Optical Parameters of the U-2 Ocean Color Scanner Channels

Channel	Center Wavelength, nm	Full Bandwidth at Half Intensity, nm	Spectral Radiance (Ocean Targets), $\text{mw cm}^{-2} \text{sr}^{-1} \mu\text{m}^{-1}$	Calibration Function Slope, $\text{mw cm}^{-2} \mu\text{m}^{-1} \text{sr}^{-1} \text{V}^{-1}$
1	431	24.2	25.54	7.298
2	472	26.0	20.94	5.984
3	506	25.0	13.49	3.853
4	548	26.3	8.276	2.365
5	586	24.1	6.334	1.810
6	625	25.3	5.007	1.430
7	667	24.2	3.883	1.110
8	707	26.0	3.167	0.9049
9	738	24.0	40.33	11.52
10	778	26.1	2.146	0.6131

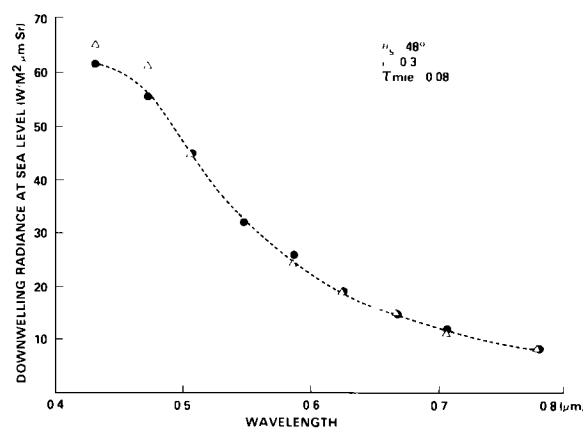


Fig. 1. A measurement (triangle) of downward atmospheric radiance by the use of U-2/OCS is compared with the calculated values (dots).

curve for a given  $\tau_{\text{mic}}$ . This can be interpreted as an indication of the instrument's reliability.

The calculation of the downwelling radiance was performed by using a plane-parallel model of the atmosphere which was originally developed by Dave [1972]. Values of the solar irradiance constants ( $F_{\lambda}^0$  in  $\text{W/m}^2 \mu$ ) used to compute the absolute radiance at the OCS wavelengths were taken from Thekaekara's table [Thekaekara, 1974] and Labs and Neckel's table [Labs and Neckel, 1968].

#### FIELD EXPERIMENTS

The U-2/OCS and the two other replicas have been frequently flown to study the oceans surrounding continental North America and western Europe. These flights were performed in support of various ocean studies. Some of the ocean features being observed were quite visible even in raw data form (i.e., quick look analog tape images of acid dumps in the New York Bight and the Red Tide (*Gymnodiniums Brevi*) blooms in the Gulf of Mexico). However, in the cases presented here, the chlorophyll feature was not immediately visible in raw data form, and additional image enhancement processing accompanied by the atmospheric effects correction was needed to bring out the feature.

In the early stages of the OCS project, it became apparent that extraction of the chlorophyll signature from field data was exceedingly complicated and, in some cases, it was totally impossible owing to the extenuating extrinsic factors influencing the ocean radiance measurement.

Therefore, it was necessary to develop a coherent analysis technique applicable to interpret data obtained under a set of appropriate weather and ocean conditions. Therefore, recent U-2/OCS flights were set to view the oceans according to the following rules:

1. First, the OCS data were taken only over the deep and the clear water of the open ocean. It has been observed that the reflection of light from the ocean floor and the scattering by sediment would strongly interfere with the chlorophyll absorption signature. A reliable method of treating underwater radiative transfer processes for turbid ocean water is not well established as of this writing. Until one can specify the light scattering properties of various phytoplankton and marine sediments with arbitrary size distribution, only the open ocean color with relatively few impurities under a near Rayleigh sky is dealt with in the present analysis.

2. Second, care was taken to collect overflight data totally

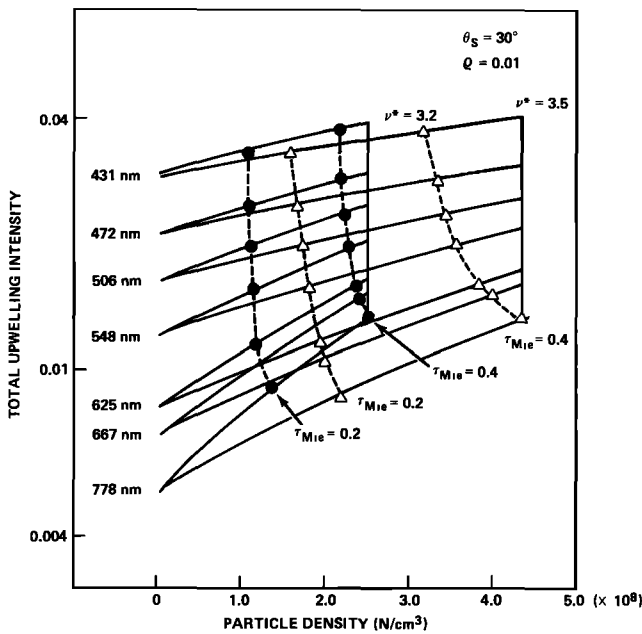


Fig. 2. Upwelling intensity for each OCS channel is plotted against aerosol content showing radiance differences owing to the aerosol size distributions,  $\nu^* = 3.2$  (dots) and  $3.5$  (triangles). The calculations are for nadir viewing normalized to a solar zenith angle of  $30^\circ$  and ground reflectivity of 1%.

free from sun-glint on the ocean surface. The sun-glint from the ocean surface is a substantial effect which will obliterate any information about the content of the subsurface phenomena. Even though the nature of sun-glint and its propagation patterns on airborne imagery are well understood [Cox and Munk, 1956; Plass et al., 1976] the removal of its effects from ocean color data usually do not allow the isolation of true water radiance from others. Therefore, it was determined that glint must be avoided by flying the aircraft directly toward or away from the sun and, at the same time, maintaining a solar zenith angle within a range of  $35^\circ$ – $60^\circ$  for optimum conditions.

3. To minimize the atmospheric effects, the data were taken only when the sky was clear and the surface of the ocean was relatively free of white caps.

4. Last, overflight data became useful only when supporting sea truth was properly collected. The ocean chlorophyll distribution can be a rapidly changing phenomena depending on the particular oceanic system being studied, and variability encompasses not only horizontal but also vertical patterns. To establish the quantitative relation of remotely sensed data with nature, the in situ measurements should be made at a precise location within a few hours of the time of the overflight. Since the U-2/OCS pixel size is on the order of  $(69 \text{ m})^2$ , the ship's absolute position must be known within a hundredth of a minute. Chlorophyll concentration and other pertinent ocean data must be taken at the surface and at several depths to give a vertical profile as well as a large area horizontal distribution pattern. The shipborne surface truth gathering activity is the most important and difficult requirement to meet in practice. It has taken several years to generate an ideal flight data set and to repeat similar experiments to verify the initial success. The first successful data were obtained during the Monterey Bay Biological Experiment which was performed in May and in September 1977. An opportunity for a second open ocean chlorophyll experiment did not materialize

until a pre-Georgia Bight Experiment (GABEX) took place off the coast of Jacksonville, Florida, in the spring of 1979.

#### ATMOSPHERIC EFFECTS CORRECTION

Essentially, the upwelling radiance measured at the U-2/OCS altitude has two primary components: (1) photons that have not penetrated the sea surface but are returned to the sensor from the atmospheric path and sea surface backscattering and (2) photons that indeed penetrated the sea surface resulting in signatures which are associated with the water and its chlorophyll concentration. The upwelling intensity in the visible channel,  $I_{\lambda_i}^{\text{total}}$  can be expressed as

$$I_{\lambda_i}^{\text{total}} = I_{\lambda_i}^{\text{atm\&sf}} + I_{\lambda_i}^{\text{water}} \quad (1)$$

Separating these two components, the  $I_{\lambda_i}^{\text{water}}$  from the  $I_{\lambda_i}^{\text{atm\&sf}}$  is difficult. In practice, the upwelling and the downwelling intensity of the sun and the diffused skylight is frequently measured by surface crews using radiometers. However, no such measurements were taken during the OCS flight in the spring of 1979.

As an alternate approach, the use of the upwelling radiance in the near-infrared channel for estimating atmospheric effects was proposed earlier and has been studied recently [Gordon, 1978]. Ocean water is nearly opaque to near-infrared radiation, and the upwelling intensity in the infrared region,  $I_{\lambda_i}^{\text{total}}$ , is simply

$$I_{\lambda_i}^{\text{total}} = I_{\lambda_i}^{\text{atm\&sf}} \quad (2)$$

(as  $I_{\lambda_i}^{\text{water}}$  is small). By modeling the upwelling radiances in both the visible and the near-infrared regions, one can derive a proportionality constant  $\eta_{\lambda_y}$ . This constant can then be applied to observations on a pixel by pixel basis to correct the atmospheric perturbations imposed upon the visible radiation. We have

$$\eta_{\lambda_y} = \frac{I_{\lambda_y}^{\text{atm\&sf}}}{I_{\lambda_x}^{\text{atm\&sf}}} \quad (3)$$

Then the true water radiance (or subsurface radiance) term at each pixel can be obtained by

$$I_{\lambda_i}^{\text{water}} = I_{\lambda_i}^{\text{total measured}} - \eta_{\lambda_y} \cdot I_{\lambda_x}^{\text{total measured}} \quad (4)$$

The method defined in (4) is essentially an inversion analysis technique, in which the ocean radiance and its wavelength dependence are derived from the measured total upward radiance and the calculated atmospheric radiance. This method assumes well-defined radiance values for the atmospheric contribution. While several numerical methods exist for the calculation of radiation transfer in the atmosphere, modeling of the upwelling radiance was carried out by using a proven method developed by J. V. Dave. In this method the radiative transfer equation for a given atmosphere model is solved by decomposing it into a series of mutually independent integrodifferential equations. Each of these equations is then solved by dividing the atmosphere into a finite number of layers and using a Gauss-Seidel iterative procedure to integrate over optical depths as was first described by Herman and Browning [1965]. The method can be used to compute the intensity of upwelling radiation in an atmosphere bounded at the bottom by a sea surface of assumed reflectivity.

To apply this ocean-atmosphere radiance computation method, the conditions under which the data were taken must

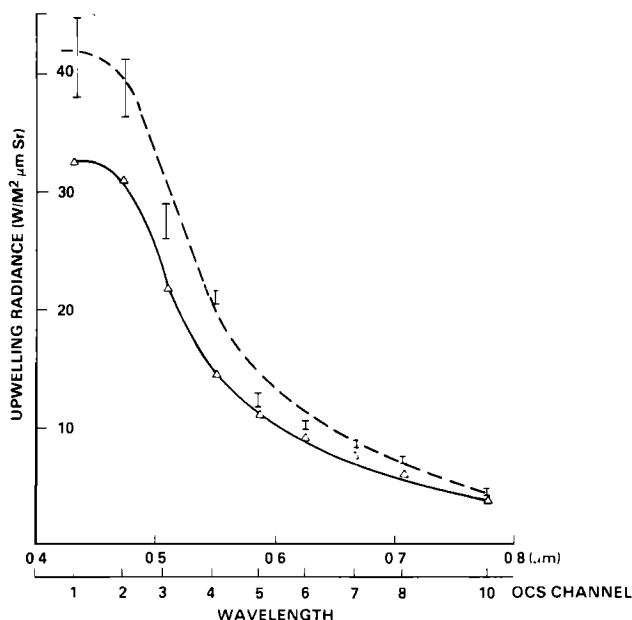


Fig. 3. Plots of upwelling radiance at nine OCS channels. Bars are actual OCS data taken from U-2 flight off Jacksonville, Florida. The solid curve indicates calculated radiance of the atmosphere and surface reflection, and the dotted curve corresponds to calculated radiance which includes the radiance contribution of ocean subsurface layer.

be scrutinized and the correct physical parameters must be incorporated into the transfer equations. The following parameters must be incorporated into the calculations:

1. The solar zenith angle.
2. Sea surface reflectivity.
3. The optical thickness of the atmosphere.
4. Refractive index and size distribution of the aerosols.

These define the aerosol single scattering phase function and single scattering albedo.

Using the Dave computer programs, one can generate radiation data points for an extensive assortment of atmospheric models. These solutions can then be specifically applied to the particular ocean scene under investigation.

In our analysis the computation of  $\eta_{\lambda}$  was performed only for the nadir observation point ( $\mu = 1$ ) and for an altitude of 19.8 km at each of the OCS channels. The aerosol single scattering phase function was calculated by using Mie theory, assuming a Junge size distribution given by

$$dN/dr = Cr^{-(\nu^*+1)} \quad (5)$$

where  $\nu^*$  values of 3.2 and 3.5 were assumed.

Also, for convenience, the real component of the aerosol refractive index was assumed to be  $M_r = 1.5$ , and the imaginary part  $M_i$  was set at zero. The reflectivity of the ocean was assumed to be 1% even though the nominal Fresnel reflectivity of the air-sea interface is 2%. The ocean surface reflection is never fully Lambertian, which makes use of the laws of diffuse reflection and transmission, but it is assumed so in the Dave programs to derive ground albedo dependent expressions after Chandrasakhar. Therefore, in the absence of direct sun-glint into the scanner field of view, the ocean surface reflectivity can be assumed much less than 2%.

A graphical plot showing the upwelling intensity in each of the Ocean Color Scanner channels as a function of aerosol content for size parameters  $\nu^* = 3.2$  and 3.5 is shown in Fig-

ure 2. The plots are for a solar zenith angle of 30°, and the ordinate intensities were calculated by using unity as the value of solar flux at 80 km above the earth's surface.

The parameter  $\eta_{\lambda}$  is derived from Figure 2 in the following manner. After selecting the appropriate size parameter which is assumed to be applicable to the particular scene being analyzed the particle number density and effective  $\tau_{Mie}$  are read from the graph for the 778 nm radiance of the scene. The effective  $\tau_{Mie}$  defines the aerosol load of the atmosphere. Then the upward atmospheric densities  $I_{\lambda}^{atm\&sf}$  of the other channels can be read from the graph for the same particle density. The parameter  $\eta_{\lambda}$  for each channel is then determined from (3). The curves in the figure represent the isolines of constant optical thickness. The lines show that wavelength dependency of  $\tau_{Mie}$  for each size distribution  $\nu^* = 3.2$  (dots) and 3.5 (triangles).

From the figure it can be seen that the error depends strongly upon estimation of the optical thickness at 778 nm and on the assumptions one has to make about the size parameters of the aerosols. To minimize the error of estimating the  $\tau_{Mie}$  at 778 nm, a high gain broadband infrared channel with a better signal-to-noise performance will be desirable for future systems. The error in approximating the size distribution of the aerosols in the atmosphere may be decreased by an interpolative readout method and by knowing the size parameter. A method to derive empirically the Junge parameter from Angstrom's wavelength exponent formula has been discussed in earlier work by Kim *et al.* [1980].

#### DERIVATION OF THE WATER RADIANCE FROM OCS DATA

The color of the ocean is truly diverse; almost any color of the spectrum can be observed from the ocean under appropriate conditions. That means there will be differences in absolute spectral radiance measured from one place to another depending on atmospheric conditions, water depth, its content, and sea state.

We have observed many different curves of spectral radiance for various locations. From the circumstances, our experimental studies have been narrowed down to the albedo of the open ocean where the absorption of blue light by the chlorophyll will shift the pure blueness to a somewhat greenish color. Typical absolute spectral radiance of the open ocean should have curves which climb almost monotonically from the near infrared into the blue where the maximum radiance occurs at 430  $\mu\text{m}$ . It should be noted that typical upwelling

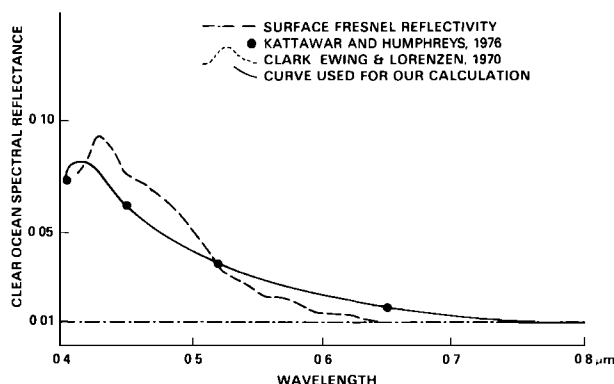


Fig. 4. Plots of clear ocean albedo showing their wavelength dependency. Solid curve profile was used for our calculation.

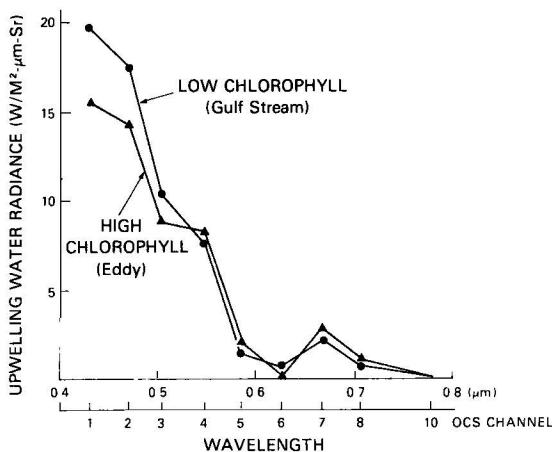


Fig. 5. Derived water radiance from OCS data: The spectral feature from low chlorophyll concentration (circle and interconnecting curve) and high chlorophyll zone (triangle and interconnecting curve).

spectra from turbid water in the coastal zones should have pronounced differences in the middle wavelength regions of the visible spectrum between 500 and 650 nm.

Therefore, the OCS flight data were carefully examined to see if the water radiance is affected by variations in hydrosols or bottom reflectance. Only those spectral curves which were obtained at nadir in the absence of any noticeable sun-glint were considered as true ocean color.

In Figure 3, curves representing absolute spectral radiance

produced by total upwelling from the ocean and the atmosphere are shown. The bars in the figure represent the actual measured radiance of nine OCS channels showing the range of values for 2500 pixels taken at the nadir-look angle. The original data were taken at the Gulf Stream front off Jacksonville, Florida. Water depths varied from 40 to 200 m, and the data were taken in midafternoon on an essentially clear day.

The measured upwelling spectral radiance at 778 nm was about  $4.8 \text{ w/m}^2/\mu\text{m}/\text{sr}$ , and this figure corresponds to a surface albedo of 0.01 according to our clear sky radiance model. Therefore, the upwelling intensity calculations for all wavelengths were performed for a 1% surface reflectivity. The results of the computations of  $I_{\lambda}^{\text{atm\&sfrc}}$  are shown by triangles and by solid curves in the figure. To locate a theoretical spectral curve which closely matches with the OCS measurement bars in the figure, the water radiance was added to the surface reflectivity already given as 1%. We assumed the clear ocean radiance model given by *Kattawar and Humphreys* [1976]. Clark et al. also has shown similar empirical spectral features in their original ocean color work. The outcome of our computations, using albedo slope given by the solid curve in Figure 4, is shown by the dotted curve in Figure 3. This maneuver is necessary to confirm the validity of the assumptions being made to construct a clear ocean radiance model.

Once the shape of the spectral plot of ocean radiance has been identified, (4) can be applied on a pixel by pixel basis. The resultant spectral features of true water radiance at high and low chlorophyll concentrations are given in Figure 5. These spectral features are different from those of the true

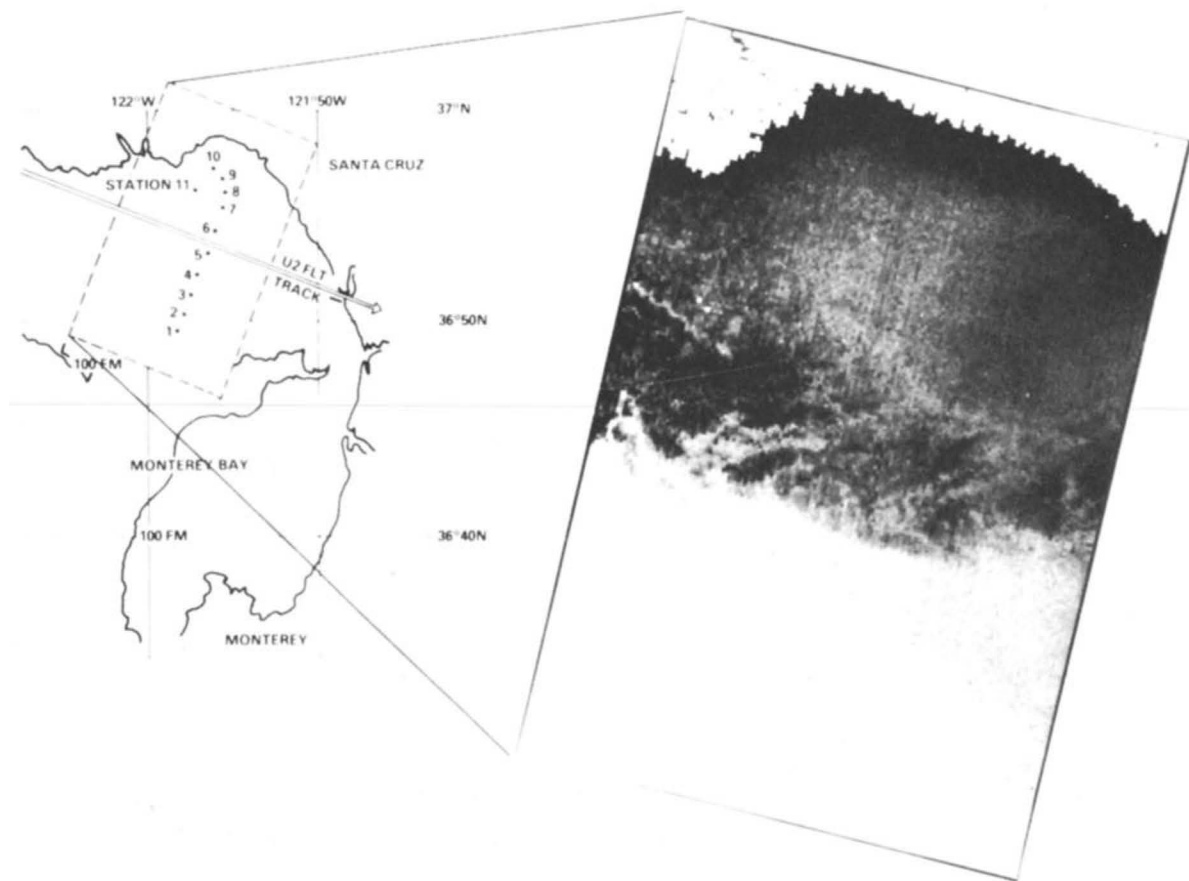


Fig. 6. A composite of auxiliary map and computer-enhanced chlorophyll gradient image of the dotted area off the coast of Monterey Bay, California.

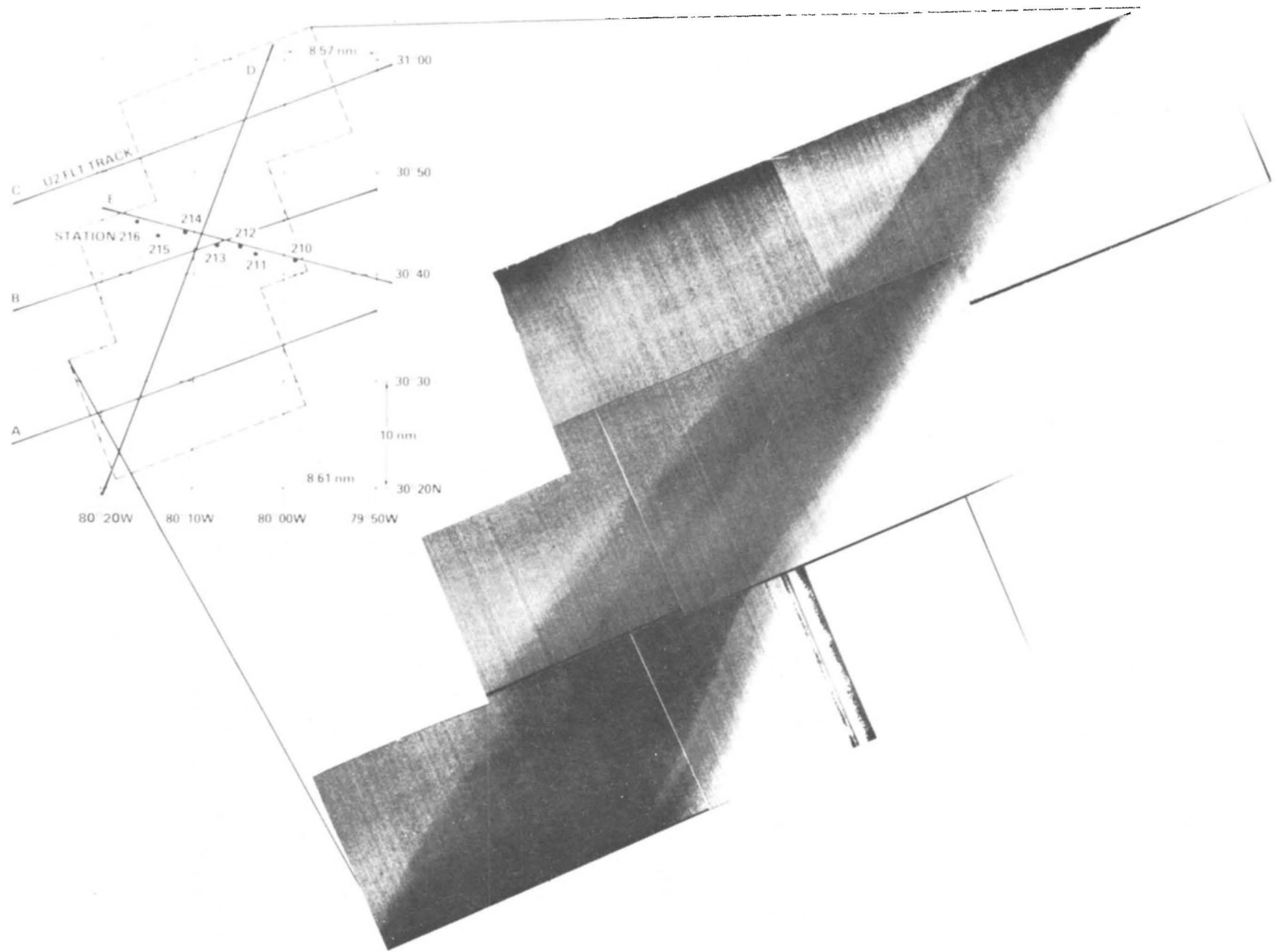


Fig 7. Similar composite as Figure 6. In developing this composite figure, atmospheric effects correction algorithms which take into account scan angle dependent contributions were used to diminish the effects of the limb-brightening on the image.



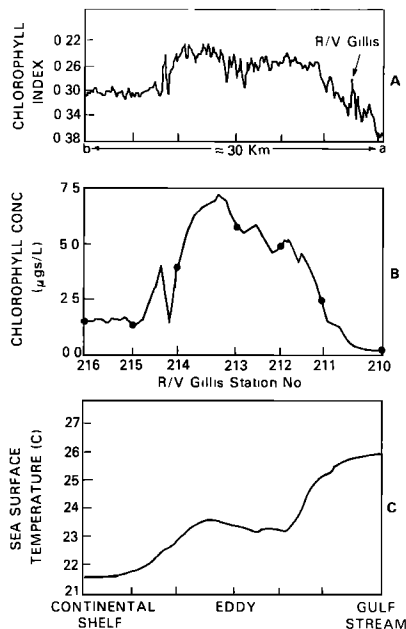


Fig. 8. (a) Chlorophyll index derived from OCS data, (b) a trace of the chlorophyll concentration, and (c) sea surface temperature as measured by the ship over the ship track E. The numbers along the bottom of Figure 8b indicate ship station numbers. Sighting of the R/V *Gillis* is shown by arrow in Figure 8a.

natural upwellings recorded at the immediate surface. Instead, they represent the water radiance that can be perceived at a 20 km height. The top trace belongs to the upwelling radiance of the ocean area where the chlorophyll concentration was reported as  $0.2 \mu\text{g/L}$  at a 2 m depth and the corresponding chlorophyll value of the lower trace was  $7 \mu\text{g/L}$ , respectively. Interestingly, the curves in Figure 5 resemble the theoretical water radiance plots, minus the white cap contributions, given by *Quenzel et al.* [1978].

#### CHLOROPHYLL ANALYSIS AND VALIDATION OF THE RESULTS WITH IN SITU MEASUREMENTS

A number of authors have demonstrated the influence of chlorophyll content on the shape of water spectra and have utilized these features for remote sensing [*Arvesen et al.*, 1973; *Grew*, 1973; *Viollier et al.*, 1978]. Most of these studies link the chlorophyll concentration in the ocean with changes in the upwelling radiation in two wavelength bands: one in the 450–500 nm region; the other in the green region between 525 and 540 nm. Recently, the successful extraction of chlorophyll information from spectral bands near 685 and 662 nm have been reported [*Neville and Gower*, 1977; *Wilson et al.*, 1978]. Two sets of U-2/OCS data have provided opportunities to verify the ability of the described analysis technique to detect variations in chlorophyll content in deep ocean water. The first of these data sets was obtained during a Monterey Bay Biology Study Experiment which was conducted jointly by Oregon State University, the U.S. Naval Post-Graduate School, and NASA/GSFC teams. The second data set was obtained from a U-2/OCS flight in support of a pre-Georgia Bight Experiment (GABEX) cruise. This experiment was conducted in the Atlantic coastal waters near Jacksonville, Florida, by L. Atkinson (Skidaway Institute of Oceanography) and associates from Skidaway, University of Miami, and

North Carolina State University. The analysis technique consisted of first determining the ocean spectral radiance from OCS data by applying a correction to eliminate the obscuring effects of the atmosphere. This involved the use of (1)–(4). After the ocean radiance was obtained for two OCS channel wavelengths, 472 and 548 nm, the following ratio was calculated:

$$R = \frac{I_{472 \text{ nm}}^{\text{water}} - I_{548 \text{ nm}}^{\text{water}}}{I_{472 \text{ nm}}^{\text{water}} + I_{548 \text{ nm}}^{\text{water}}} \quad (6)$$

The ratio  $R$  is referred to as the chlorophyll index. These particular spectral bands were chosen because, as indicated in Figure 5, light at 472 nm is highly affected by chlorophyll absorption while light at 548 nm is minimally affected. The chlorophyll index was calculated on a pixel by pixel basis for selected scenes derived from OCS data from the two experiments mentioned above. Computer-produced images of the chlorophyll index from these scenes were made and were recorded on photographic film. These images represented areal maps of the chlorophyll gradients within the boundaries of the scenes in Figure 6 and Figure 7. Areas of relatively high chlorophyll concentration were represented by darker areas on the photograph, while low concentration was represented by lighter areas. Figure 6 is an image of chlorophyll index produced from the Monterey Experiment. Comparison of the chlorophyll index  $R$  with the chlorophyll concentration  $C$  measured by a surface vessel at the 11 points shown on the image indicates, as was expected, a distinct negative relationship between the  $R$  and the  $C$ . On the left of the scene the flow of the California current, which is low in bioproductivity, is made evident by the light shade of the ocean. This data set was the first in which it was possible to confirm the validity of the described concept of chlorophyll analysis [*Zaneveld*, 1978].

The second opportunity for validation was provided by the recent Florida overflight. In a carefully designed procedure, the U-2 was flown in three parallel and two skew lines covering an area of high chlorophyll concentration. This chlorophyll feature, as monitored by the R/V *Gillis*, covered an elongated area, greater than 100 km in length, located on the western edge of the Gulf Stream. A composite image of the chlorophyll index was made from the three parallel flight lines and is displayed in Figure 7. This composite clearly shows the distinct upwelling feature extending from top to bottom on the image. The feature separates the shelf water on the left from the infertile Gulf Stream on the right. Flight line E was approximately  $18^\circ$  to the solar plane and was coincident with the R/V *Gillis* track as it proceeded from the Gulf Stream over the chlorophyll maximum to the shelf. A trace of the concentration as measured by the ship is shown in Figure 8b. Above this trace, in Figure 8a, is the trace of the chlorophyll index  $R$  derived from the OCS as it covered the same course as the ship but 2–3 hours prior to the ship's transect. The numbers along the bottom of Figure 8b indicate ship stations where the location of the ship and chlorophyll concentration are precisely known. The two traces show good agreement in the location where the concentration is low or moderate; that is, where the chlorophyll concentration is below about  $10 \mu\text{g/L}$ . At concentrations above this amount, the index loses sensitivity. Absorption of the blue light by the chlorophyll pigment varies as an inverse exponential of the concentration and thus, as the concentration becomes larger, variation of absorption becomes less sensitive to variation of concentration. Hence,

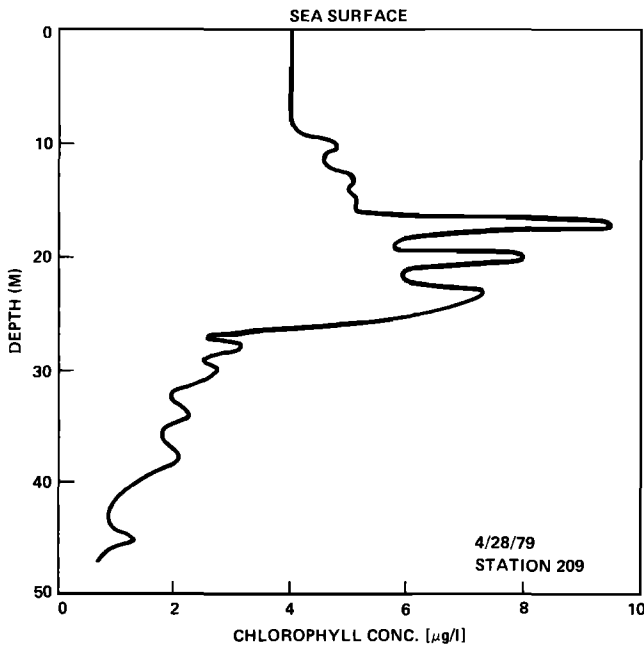


Fig. 9. Vertical distribution of chlorophyll at Gillis station 209 just south of transect E.

the peak in concentration as detected by the ship is not clearly distinguishable in the trace of the index.

On the other hand, a sharp minor peak in the chlorophyll concentration between stations 214 and 215 is very distinctly seen in the trace of  $R$ . A point of interest is the peak in the trace of  $R$  between stations 210 and 211. This peak is an anomaly which resulted when the U-2 had the research vessel in its view. This fortuitous sighting permitted accurate mapping of the ship track on the OCS image. Figure 8c shows the change in the sea surface temperature along the track indicating a rather weak thermal signature. To provide an idea of the vertical chlorophyll distribution, Figure 9 is shown. It indicates a large subsurface peak 15–25 m down, but the top 15 m is quite uniform.

A plot was made of the chlorophyll concentration  $C$  and the chlorophyll index  $R$  for the seven station locations from the Atlantic experiment (triangles) and five deep-water spots from the Pacific Ocean (crosses). This plot is shown in Figure 10. A

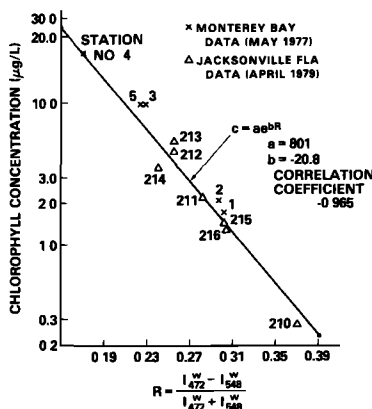


Fig. 10. Correlation between the measured chlorophyll concentration  $C$  and the derived products  $R$  by taking the ratio of  $I_{472}$  nm and  $I_{548}$  nm is shown. The calculated correlation coefficient for the points was  $-0.965$ .

least squares method was used to fit the data with a line of the following form

$$C = ae^{bR} \quad (7)$$

The coefficients  $a$  and  $b$  were determined to be 801 and  $-20.8$   $\mu\text{g}/\text{L}$  respectively. The correlation coefficient for the points in  $\ln(C)$  versus  $R$  was  $-0.965$ . It would be desirable to establish a universal quantitative relationship between the chlorophyll concentration  $C$  and  $R$ , or some other parameter produced from remote sensed data. This would require repeated field experiments so that a library of data could be developed.

Earlier efforts to use U-2/OCS data have been hampered because the data were generally obtained in coastal regions. Coastal color phenomenology is extremely complex and multifaceted. The utilization of the analysis technique that has been described could not be demonstrated in a specific application owing to the lack of a reliable underwater radiative transfer process modeling method which could deal with the light scattering properties of hydrosols. For these reasons the authors have limited the scope of this study to conditions of clear water in open ocean areas. The results of the study confirm the validity of the approach.

Thus far the results of the study indicate that the application of this colorimetric technique for bioresources remote sensing is well suited to open ocean studies. As exhibited in the correlation plot of Figure 10, chlorophyll measurement is easiest when concentrations are in the low  $\mu\text{g}/\text{L}$  range. This is because the upwelling radiance changes owing to the chlorophyll concentration is an exponential function, and the quantizing range of the instrument will determine the upper limits of resolvable chlorophyll concentration. The data show that the chlorophyll concentration can be determined up to the 10  $\mu\text{g}/\text{L}$  level with reasonable accuracy and reliability. Chlorophyll distribution patterns in the open ocean are an important indication of changes in water type which reflect the circulation and anomalies associated with the main flow, such as regional upwelling phenomena or meandering eddies. The subtle differences in chlorophyll content in large water bodies of different origins can be recognized by this ocean colorimetric technique. For these reasons it is desirable that further study be conducted to obtain more comprehensive data sets so that the analysis algorithms can be further improved.

**Acknowledgment.** The authors wish to thank R. S. Fraser for helpful discussions concerning the atmospheric radiance.

## REFERENCES

- Arvesen, J. C., J. P. Millard, and E. C. Weaver, Remote sensing of chlorophyll and temperature in marine and fresh waters, *Astronaut. Acta.*, 18, 229–239, 1973.
- Clark, G. L., C. Ewing, and C. J. Lorenzen, Spectra of backscattered light from the sea obtained from aircraft as measure of chlorophyll concentration, *Science*, 167, 1119–1120, 1970.
- Cox, C., and W. Munk, Slopes of the sea surface deduced from photographs of sun glitter, *Bull. Scripps Inst. Oceanogr.*, 6, 401–488, 1956.
- Dave, J. V., Development of programs for computing characteristics of ultraviolet radiation, *Tech. Rep. Scalar Case (SPA-D)*, NASA contract NAS5-2168, IBM, Palo Alto, Calif., 1972.
- Gordon, H., Removal of atmospheric effects from satellite imagery of the oceans, *Appl. Opt.*, 17, 1631–1635, 1978.
- Grew, G. W., Signature analysis of reflectance spectra of phytoplankton and sediment in inland waters, *Remote Sensing Earth Res.*, 2, 1147–1172, 1973.
- Herman, B. M., and S. R. Browning, A numerical solution to the equation of radiative transfer, *J. Atmos. Sci.*, 22, 559–566, 1965.
- Hovis, W. A., M. L. Forman, and L. R. Blaine, Detection of ocean

- color changes from high altitude, *NASA/GSFC X Doc. 652-73-371*, 1973.
- Kattawar, G. W., and T. J. Humphreys, Remote sensing of chlorophyll in an atmosphere-ocean environment: A theoretical study, *Appl. Opt.*, *15*, 273-282, 1976.
- Kim, H. H., R. S. Fraser, L. Thompson, and O. P. Bahethi, A system study of an advanced ocean color scanner, *Boundary Layer Meteorol.*, *18*, 343-355, 1980.
- Labs, D., and H. Neckel, The radiation of the solar photosphere from 2000 Å to 100  $\mu$ , *Zeit. Astroph.*, *69*, 1-73, 1968.
- Neville, R. A., and J. F. R. Gower, Passive remote sensing of phytoplankton via chlorophyll fluorescence, *J. Geophys. Res.*, *82*, 3487-3493, 1977.
- Plass, G. N., G. W. Kattawar, and J. A. Guinn, Jr., Radiance distribution over a ruffled sea: Contributions from glitter, sky and ocean, *Appl. Opt.*, *15*, 3161-3165, 1976.
- Quenzel, H., and M. Kästner, Masking effects by the atmosphere on remote sensing of chlorophyll in the ocean, Final Report, Univ. of München, Germany, 1978.
- Thekaekara, M. P., Extraterrestrial solar spectrum, 3000-6000 Å at 1 Å intervals, *Appl. Opt.*, *13*, 518-522, 1974.
- Viollier, M., P. Y. Deschamps, and P. Lecomte, Airborne remote sensing of chlorophyll content under cloudy sky as applied to the tropical water in the Gulf of Guinea, *Remote Sensing Environ.*, *7*, 187-202, 1978.
- Wilson, W. H., R. W. Austin, and R. C. Smith, Optical remote sensing of chlorophyll in ocean waters, in *Proceedings of 12th International Symposium on Remote Sensing of Environment*, pp. 1103-1113, ERIM, Ann Arbor, Mich., 1978.
- Zaneveld, J. R., J. C. Kitchen, R. Barts, D. Menzies, S. Moore, R. Spinrod, and H. Pak, Optical, hydrographic and chemical observations in the Monterey Bay area during May and September 1977, *NASA contract S-23728 report*, Oregon State Univ., School of Oceanography, Corvallis, 1978.

(Received November 9, 1979;  
revised March 24, 1980;  
accepted April 4, 1980.)